

Article

On the Heat Transfer Enhancement of Plate Fin Heat Exchanger

Yuan Xue ¹, Zhihua Ge ^{1,*}, Xiaoze Du ^{2,*}  and Lijun Yang ¹

¹ Key Laboratory of Condition Monitoring and Control for Power Plant Equipment, Ministry of Education, North China Electric Power University, Beijing 102206, China; alma19911918@126.com (Y.X.); yanglj@ncepu.edu.cn (L.Y.)

² School of Energy and Power Engineering, Lanzhou University of Technology, Lanzhou 730050, China

* Correspondence: gezh@ncepu.edu.cn (Z.G.); duxz@ncepu.edu.cn (X.D.); Tel.: +86-10-6177-3923 (Z.G.); Fax: +86-10-6177-3877 (Z.G.)

Received: 21 April 2018; Accepted: 15 May 2018; Published: 30 May 2018



Abstract: The plate fin heat exchanger is a compact heat exchanger applied in many industries because of its high thermal performance. To enhance the heat transfer of plate fin heat exchanger further, three new kinds of wavy plate fins, namely perforated wavy fin, staggered wavy fin and discontinuous wavy fin, are proposed and investigated by computational fluid dynamics (CFD) simulations. The effects of key design parameters, including that of waviness aspect ratios, perforation diameters, staggered ratios and breaking distance are investigated, respectively, with Reynolds number changes from 500 to 4500. It is found that due to the swirl flow and efficient mixing of the fluid, the proposed heat transfer enhancement techniques all have advantages over the traditional wavy fin. At the same time, serration is beneficial to reduce the friction factor, and the breaking technique can reduce heat transfer area. Through the performance evaluation criteria, the staggered wavy fin has an advantage over the small waviness aspect ratio; with increasing waviness aspect ratio, this predominance is gradually surpassed by the perforated wavy fin, and the advantage of the discontinuous fin is the smallest and almost invariable. A maximum performance evaluation criteria (PEC) as high as 1.24 can be obtained for the perforated wavy fin at the waviness aspect ratio $\gamma = 0.45$.

Keywords: staggered wavy fin; perforated wavy fin; discontinuous wavy fin; heat transfer enhancement

1. Introduction

As a compact heat exchanger, the plate fin heat exchanger is applied in many industries and occupies a unique role due to its flexible arrangement, simple shape, and good thermal effectiveness. Based on different applications, various kinds of fins are used in plate fin heat exchangers, such as plain, offset-strip, louvered, wavy and pin [1–5]. Kays and London conducted an experimental analysis of about 40 kinds of fins and offered the corresponding correlation curves of heat transfer and resistance [6]. Khoshvaght-Aliabadi investigated seven common configurations of channels used in plate fin heat exchangers experimentally. The results showed that a vortex-generator channel can be applied as a high-quality interrupted surface, and wavy channel displayed an optimal performance in low Reynolds numbers [7]. Juan Du carried out experimental and numerical investigations of the heat transfer and pressure drop characteristics of an offset plate fin heat exchangers for cooling of lubricant oil [8]. Numerical simulations and experimental study on the flow and heat transfer characteristics of air in wavy fin were carried by Dong. The results show that the waviness amplitude has a significant effect on the heat transfer and pressure drop of wavy fin [9].

More recently, there has been various research on the development of new types of fin for heat transfer enhancement [10–12], including that of offset strip fins compact heat exchanger [13], fins with

grooves or vortex generators [14,15]. El Hassan Ridouane found that the grooves on the fin surface can enhance local heat transfer significantly [16]. The numerical simulation also found that the multi-row windward punched delta winglet on the plain fin has much enhanced performance [17]. Both experiment and numerical simulations have been conducted to investigate the air-side flow and heat transfer of the wavy fin with or without delta winglet pairs punched on the surface. The results showed that the wavy fin with delta winglet pairs can significantly enhance air-side heat transfer and pressure drop [18]. Thermal characteristics of the plan and curved vortex generators with or without punching holes in the fin surface were investigated, indicating that vortex generators with holes have higher heat transfer enhancement and lower pressure drop than those without holes [19]. In order to resolve the shortcomings of the louver fin heat exchanger, Chan Hyeok Jeong developed the plate fin with both ceases and holes, which helped to improve heat transfer and could be used under hostile environments [20]. The effects of round and elongated holes were also compared [21]. It was found that the elongated holes offered better performance but also with larger pressure drops.

Among the numerous studies on the different kinds of fins, wavy and offset strip fins are the most popular ones because of their high thermal performances. Punching holes on the fin surface can enhance heat transfer significantly. However, there have hitherto been few studies regarding the effects of the staggered arrangement on wavy fins. In the present study, three new kinds of wavy plate fin configurations are considered by numerical investigations. The benefits of heat transfer and pressure drop of the plate fin heat exchanger have analyzed accordingly.

2. Physical and Mathematic Model

2.1. Physical Model

The heat transfer performance and flow resistance of four kinds of wavy plate fins are evaluated using computational numerical analysis. Figure 1 shows the shape and geometric details of the objective wavy fins. Compared with the traditional wavy fin, three enhanced configurations, shown in Figure 1b–d, were also investigated to verify their heat transfer performances, including that of the perforated wavy fin, staggered wavy fin, and discontinuous wavy fin, in which, F_h is the fin height; F_p is the fin pinch; r is the perforation radius; S is the breaking distance in discontinuous fin.

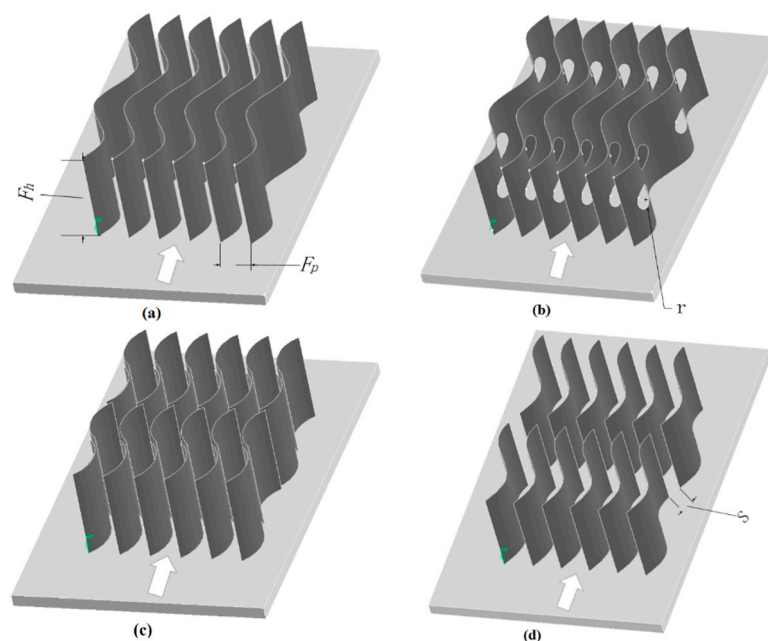


Figure 1. The shape of (a) traditional wavy fin; (b) perforated wavy fin; (c) staggered wavy fin; (d) discontinuous wavy fin.

2.2. Governing Equations

The continuity, momentum, and energy equations are listed as follows, which govern the three-dimensional, steady-state flow of air flowing in the proposed wavy fin passage.

$$\frac{\partial(\rho u_i)}{\partial x_i} = 0 \quad (1)$$

$$\frac{\partial(\rho u_i u_j)}{\partial x_i} = -\frac{\partial p}{\partial x_i} + \frac{\partial}{\partial x_j} (\tau_{ij} - \overline{\rho u'_i u'_j}) \quad (2)$$

$$\frac{\partial}{\partial x_i} (\rho u_i C_p T) = \frac{\partial}{\partial x_i} \left(\lambda \frac{\partial T}{\partial x_i} \right) \quad (3)$$

where ρ is the fluid density; u_i and u_j are the velocity in the i and j direction; x_i is the coordinate; p is the pressure, τ is the shear stress; C_p is the specific heat; T is the temperature; λ is the thermal conductivity.

In which,

$$\tau_{ij} = \mu \left(\frac{\partial u_i}{\partial x_j} + \frac{\partial u_j}{\partial x_i} - \frac{2}{3} \delta_{ij} \frac{\partial u_k}{\partial x_k} \right) \quad (4)$$

$$-\overline{\rho u'_i u'_j} = \mu_t \left(\frac{\partial u_i}{\partial x_j} + \frac{\partial u_j}{\partial x_i} - \frac{2}{3} \delta_{ij} \frac{\partial u_k}{\partial x_k} \right) - \frac{2}{3} \delta_{ij} \rho k \quad (5)$$

$$k = \frac{\overline{u'_i u'_j}}{2} \quad (6)$$

in which, μ is the dynamic viscosity; μ_t is the turbulent viscosity; δ_{ij} is the Kronecker delta; k is the turbulence kinetic energy.

The standard $k - \varepsilon$ model, low Re $k - \varepsilon$ model, RNG $k - \varepsilon$ model and $k - \omega$ SST model are used as turbulent models for verification of calculation, finally, the RNG $k - \varepsilon$ is selected because of the minimum error between the results and reference experimental data (For details, see Section 3.1). For the RNG $k - \varepsilon$ model, the turbulence kinetic energy, k , and dissipation rate, ε , are calculated as,

$$\frac{\partial}{\partial x_i} (\rho k u_i) = \frac{\partial}{\partial x_j} \left[\left(\mu + \frac{\mu_t}{\sigma_k} \right) \frac{\partial k}{\partial x_j} \right] + G_k - \rho \varepsilon \quad (7)$$

$$\frac{\partial}{\partial x_i} (\rho \varepsilon u_i) = \frac{\partial}{\partial x_j} \left[\left(\mu + \frac{\mu_t}{\sigma_\varepsilon} \right) \frac{\partial \varepsilon}{\partial x_j} \right] + C_{1\varepsilon} \frac{\varepsilon}{k} G_k - C_{2\varepsilon} \rho \frac{\varepsilon^2}{k} \quad (8)$$

and with the model constants as $C_{1\varepsilon} = 1.42 - \frac{\tilde{\eta}(1-\tilde{\eta}/\tilde{\eta}_0)}{1+\beta\tilde{\eta}^3}$, $\tilde{\eta} = Sk/\varepsilon$, $S = (2S_{i,j}S_{i,j})^{1/2}$, $S_{i,j} = \frac{1}{2}(\frac{\partial u_i}{\partial x_j} + \frac{\partial u_j}{\partial x_i})$, $\tilde{\eta} = 4.38$, $\beta = 0.015$, $C_{2\varepsilon} = 1.68$, $\sigma_k = 0.7179$, $\sigma_\varepsilon = 0.7179$. μ_t and G_k denote turbulent viscosity and the generation of turbulence kinetic energy because of the mean velocity gradients.

Figure 2 shows the geometric details, computational domains and the boundary conditions for staggered wavy fins, where the regions enclosed by the dashed lines are designated as computational domains of the staggered wavy fins. The boundary conditions consist an inlet, an outlet, the periodic left and right, and the boundary condition of plate part is constant wall temperature that is 334 K.

It is illustrated in Figure 2 that F_c is the staggered spacing; l is the wavy length; a is the wave amplitude.

In order to ensure the uniformity of air inlet velocity, the length of the upstream zone is taken 30 mm and the length of the downstream is extended to 100 mm to avoid the flow recirculation at the outlet. The boundary condition of computational domain inlet is defined as the velocity inlet, the velocity is from 5 to 25 m/s, and the constant air inlet temperature is 398 K.

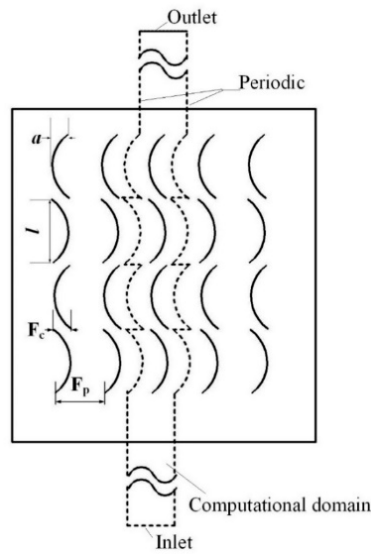


Figure 2. Computational domains and boundary details for the staggered wavy fin.

2.3. Parameter Definitions

For the heat transfer performance, the air-side surface heat transfer coefficient, h , of the wavy fin is calculated as follows,

$$h = \frac{Q}{A \cdot \Delta T} \quad (9)$$

$$\Delta T = \frac{(T_{in} - T_w) - (T_{out} - T_w)}{\ln[(T_{in} - T_w)/(T_{out} - T_w)]} \quad (10)$$

$$Q = mC_p(T_{in} - T_{out}) \quad (11)$$

where m , C_p , T_{out} , T_{in} are the mass flow rate of air flow, specific heat, inlet and outlet bulk temperatures of air, respectively. T_w is the bottom wall temperature which is a constant, 334 K. A is the total heat transfer area of the plate and effective wavy fins. $A = A_p + \eta_f A_f$, of which, A_p is the plate surface, A_f is all fin surface that contact with air. $\eta_f = \frac{T_{f,ave} - T_{air,ave}}{T_w - T_{air,ave}}$ is the fin efficiency with $T_{air,ave} = \frac{1}{2}(T_{in} + T_{out})$.

The Reynolds number is defined as

$$Re = \frac{GD_h}{\mu} \quad (12)$$

in which, G is the mass velocity, D_h is the hydraulic diameter for the plate staggered wavy fin channel given by Ref. [22].

$$D_h = \frac{4A_c L}{(A_p + A_f)} \quad (13)$$

where A_c is the minimum free flow area, L is the flow length.

For the proposed wavy fin studied in current study, D_h is given as

$$D_h = \frac{2(F_p - \delta)F_h L}{(F_p L + F_h L_z - \pi r^2)} \quad (14)$$

where δ is the fin thickness, L_z is the wavy fin passage length.

The specific geometrical feature of the wavy fin is described by the wave amplitude (a) and wavelength (l). The waviness aspect ratio is defined as

$$\gamma = 2a/l \quad (15)$$

For the staggered wavy fin, the staggered ratio is described as

$$\beta = F_c / F_p \quad (16)$$

where F_c is the staggered spacing.

The mean Nusselt number is described as

$$Nu = \frac{hD_h}{\lambda} \quad (17)$$

The Colburn factor and Fanning friction factor are defined as

$$j = \frac{Nu}{RePr^{1/3}} \quad (18)$$

$$f = \frac{\rho D_h \Delta P}{2LG^2} \quad (19)$$

where ΔP is the pressure drop between the inlet and outlet of the air channel.

For the comparison of the overall flow and heat transfer performance of the proposed wavy fins, the heat exchanger performance evaluation criteria (PEC) is defined as

$$PEC = \frac{Nu / Nu_{basic,wavy}}{(f / f_{basic,wavy})^{1/3}} \quad (20)$$

2.4. Grid Independence Tests and Verification of CFD Model

The mathematical model of the turbulent flow through the wavy fin is solved by using the commercial software FLUENT developed by ANSYS, Canonsburg, PA. The second-order upwind scheme is used to solve the momentum and energy equations. The pressure-velocity coupling flow analysis is conducted using a SIMPLE algorithm.

The computational meshes are generated by software GAMBIT 2.4.6 developed by ANSYS, Canonsburg, PA. For the region of computational domains, the structured mesh is used. For the periodic boundary, the meshes are matched by linking the periodic surfaces.

Grid independence tests are carried out before further numerical work to validate the independence of solution on the grid number. Three different grid numbers are employed to check the influence of the grid number, which includes about 1,159,000, 1,600,000, and 1,930,000 cells. Figure 3 shows the change in the j factor in accordance with the change of grid number. As shown in Figure 3, the change of j factor is less than 5% when the grid number increased from 1.159 to 1.93 million. The more grid numbers, the more computing resources and time consuming. In order to achieve a moderate accuracy and save computation time, the calculation was conducted using the corresponding mesh division method of 1.60 million grid numbers.

Figure 4 shows the comparison between the values of the (a) j and (b) f factors using different turbulent models (standard $k - \varepsilon$ model, low Re $k - \varepsilon$ model, RNG $k - \varepsilon$ model and SST model) at Re from 1000 to 4000 for the traditional wavy fin. The values of the j and f factors on the experiment are obtained using the correlations presented by Dong Junqi [23] with the same geometric parameters. The RNG $k - \varepsilon$ is selected because of the minimum error between the results and reference experimental data.

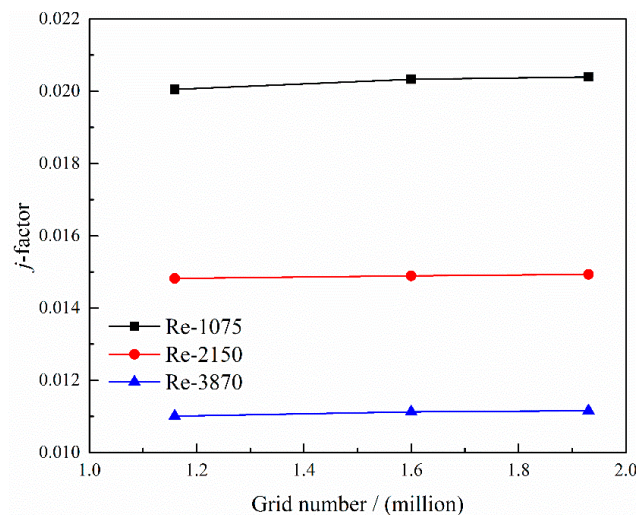


Figure 3. Change in the j -factor in accordance with the change of grids number.

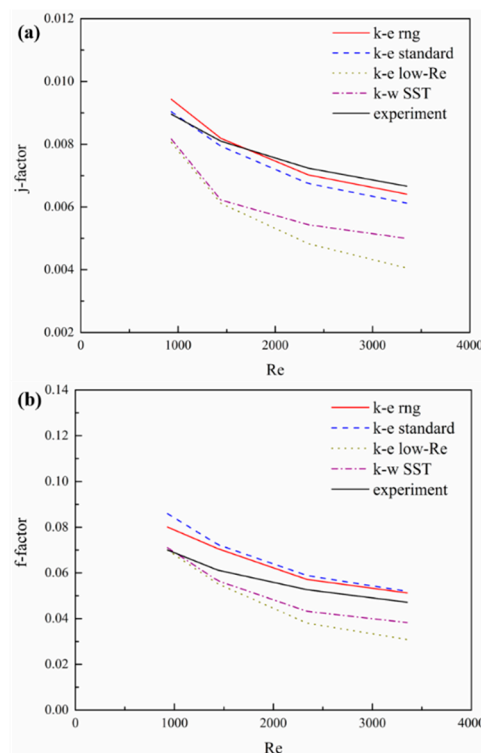


Figure 4. Comparison between the values of the (a) j -factor and (b) f -factor using different turbulent flow models.

The standard $k - \varepsilon$ model assumes that the flow is completely turbulence and the influence of molecular viscosity can be ignored. It is only suitable for the simulation of complete turbulent flow. When there is strong streamline bending, whirlpool and swirling in the fluid, the accuracy of the calculation is relatively low. The low Re $k - \varepsilon$ model considers the whole boundary layer and does not depend on the wall function. Therefore, it needs more sophisticated grids and only can be used under low Reynolds number conditions or in an area near the wall surface. The SST model has a strong dependence on the distance to the wall and is suitable for simulating the boundary layer and low Reynolds number flow. The RNG $k - \varepsilon$ theory not only takes into account the turbulence vortices but also provides an analytical formula for the viscous flow at low Reynolds numbers. These characteristics

make the RNG $k - \varepsilon$ model more reliable and accurate than other methods, which also can be seen in Figure 4. The reason for the difference between RNG $k - \varepsilon$ model and reference experimental data could be because the data is not directly from the measurement of experiment, but by the fitting formula obtained from the experiment. On the other hand, for the wavy fin, there are subtle radian differences between the fins used in the experiment and the numerical simulation models.

Therefore, the RNG $k - \varepsilon$ model is employed in the simulation. The enhanced wall function was adopted to deal with the near wall region.

3. Results with Analysis

3.1. Influence of Different Perforated Radius

The relation of the Nusselt number ratio ($Nu/Nu_{basic,wavy}$), friction factor ratio ($f/f_{basic,wavy}$) and the PEC to the Reynolds number for the different perforated radius are presented in Figure 5. Figure 6 shows the change in the streamline and fin surface temperature distribution of the perforated wavy fin with the different radius. The radii of the punched holes are 0.5 mm, 1 mm, and 1.5 mm, respectively. It can be found that at the same operating condition, the perforated wavy fin with the larger punched hole has higher values of Nusselt number and friction factor. The streamline in Figure 6a shows that the enlarged hole can strengthen the flow turbulence, causing rapid mixing between the core and the fluid near the fin surface. From Figure 6b it can be seen that for wavy fin with larger punched holes the surface temperature of most regions is higher than those with smaller holes. It means that these fins had a better heat transfer. A surface having a high PEC is advantageous because it enables a heat exchanger to have good heat transfer and pressure loss performance. It is observed in Figure 5c that the PEC for the perforated wavy fin with $r = 1.5$ mm is obviously higher than that of the others.

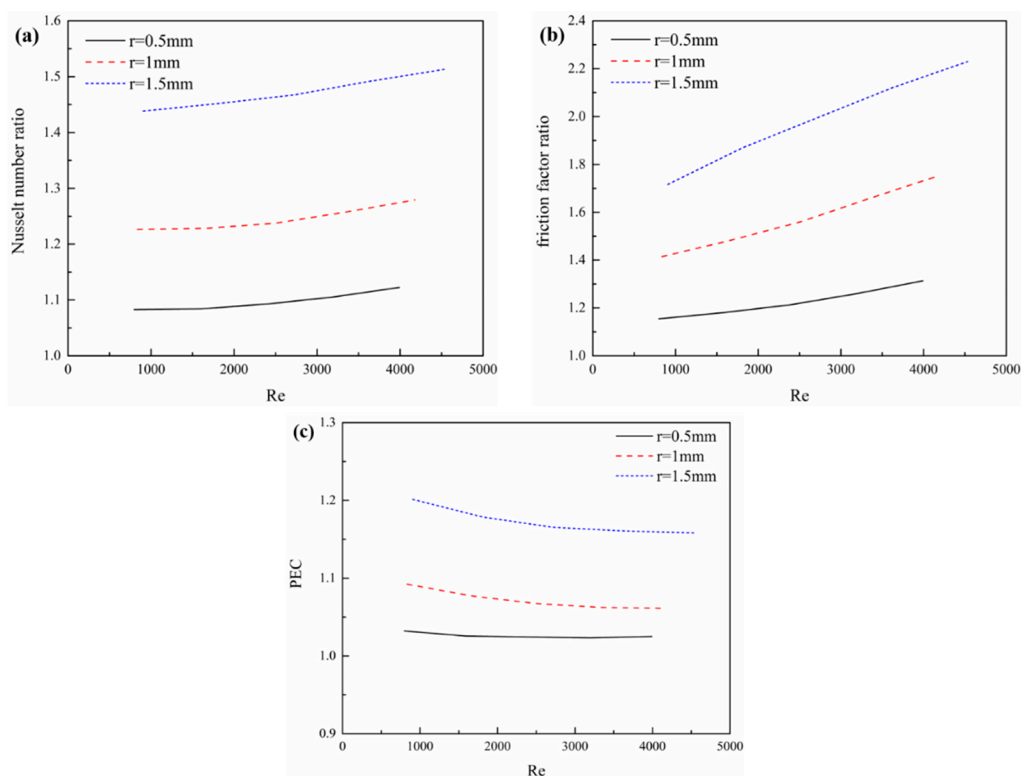


Figure 5. Influence of different perforated diameter on heat transfer performance with Reynolds number. (a) Nusselt number ratio; (b) friction factor ratio; (c) the performance evaluation criteria (PEC).

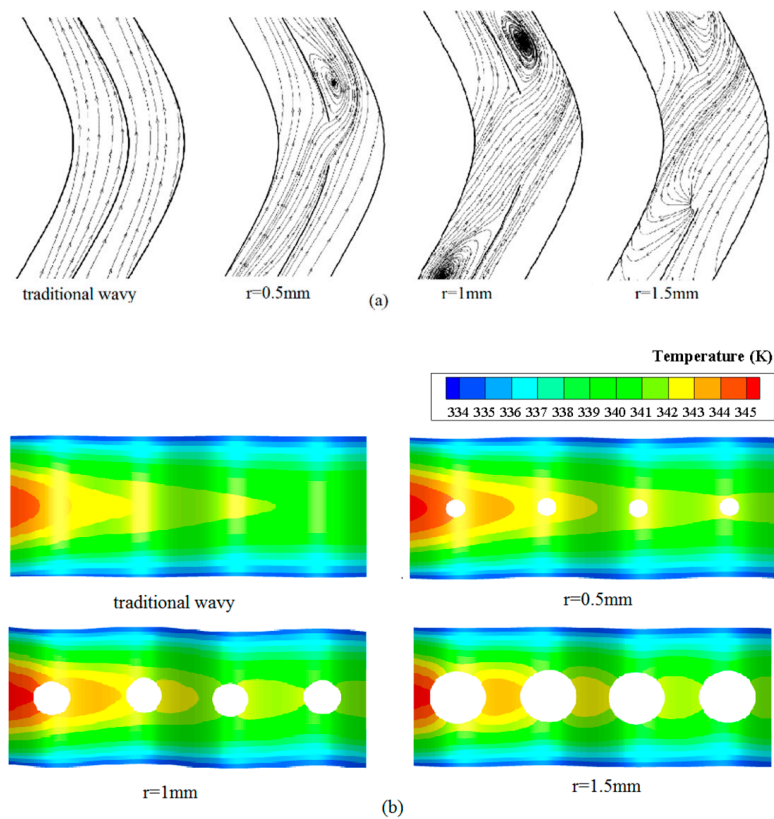


Figure 6. (a) Change in the streamline and (b) fin surface temperature distributions of the traditional wavy fin and perforated wavy fin when the radii are 0.5 mm, 1 mm and 1.5 mm.

3.2. Influence of Different Staggered Ratio

Figure 7 shows, respectively, the relations between the Nusselt number ratio ($Nu/Nu_{basic,wavy}$), friction factor ratio ($f/f_{basic,wavy}$) and the PEC under different staggered ratio. Figure 8 displays the change in the streamline, the fin surface temperature distribution of the traditional wavy fin and staggered wavy fin with the different staggered ratio. The staggered ratios are 0.2, 0.3, and 0.4, respectively. In Figure 7a, it is shown that the staggered wavy fin with staggered ratio $\beta = 0.4$ has higher values of the Nusselt number ratio, which is all greater than 1 in the simulation range. It is observed in Figure 7b that friction factor ratio of staggered wavy fin increases with the increase of the Reynolds number. It is important to note that within the simulation range, the friction factor ratio is observed to be less than 1 when Re is less than 2500. Therefore, the staggered structure is good for reducing the pressure drop. From the streamline shown in Figure 8a it can be seen that the greater staggered ratio, the less flow turbulence at the staggered section. At the same time, the increase of staggered ratio decreases the swirl flow near the fin surface which is beneficial for adequate heat transfer. As shown in Figure 8b, the larger the staggered ratio, the higher the surface temperature of the fin. Figure 7c shows that the heat exchanger performance evaluation criteria for the staggered wavy fin with staggered ratio 0.4 is obvious compared to the others within the simulation range.

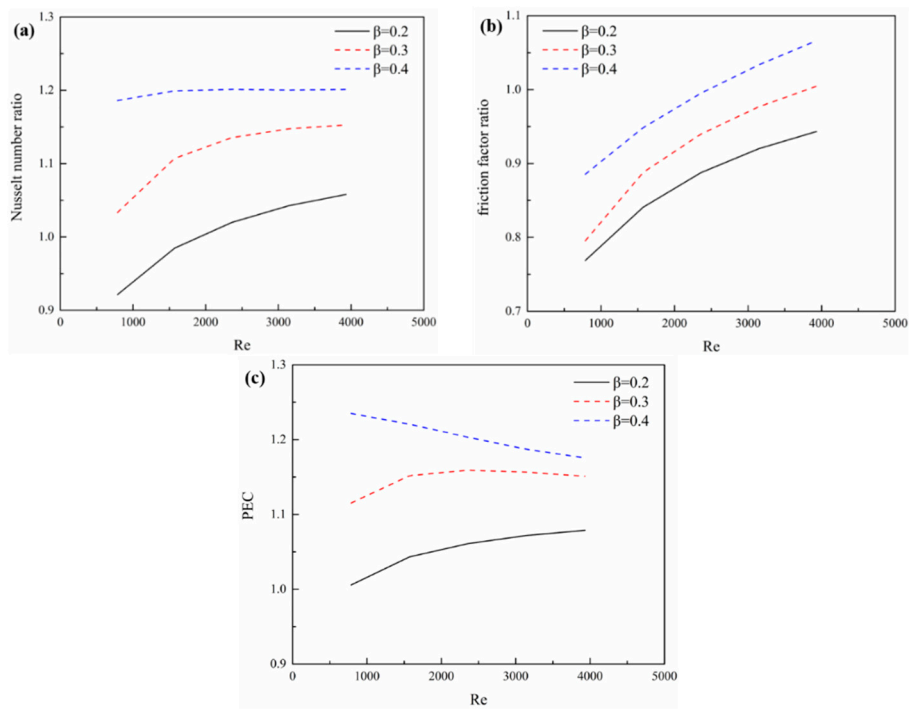


Figure 7. Influence of different staggered ratio on heat transfer performance with Reynolds number. (a) Nusselt number ratio; (b) friction factor ratio; (c) the PEC.

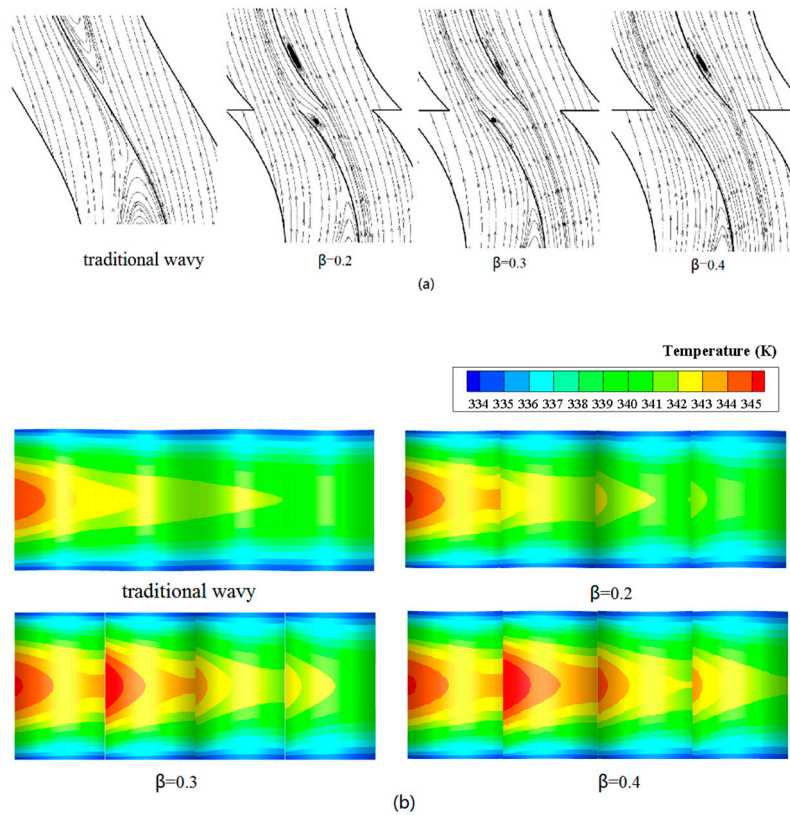


Figure 8. (a) Change in the streamline and (b) fin surface temperature distribution of the traditional wavy fin and staggered wavy fin when the staggered ratios are 0.2, 0.3 and 0.4.

3.3. Influence of Different Breaking Distance for Discontinuous Wavy Fin

Figure 9 shows the relations between the Nusselt number ratio ($Nu/Nu_{basic,wavy}$), friction factor ratio ($f/f_{basic,wavy}$) and the PEC under different breaking distance, respectively. The change in the streamline and fin surface temperature distribution of the traditional wavy fin and discontinuous wavy fin with different breaking distance is showed in Figure 10. The distances are 0.5 mm, 1 mm, and 2 mm, respectively. It is observed that the discontinuous wavy fin with large spacing has higher values of Nusselt number and friction factor. The friction factor ratio of discontinuous wavy fin increases with the increase of Re, and the slope is maximum when the breaking distance is 2 mm. The streamline shown in Figure 10a suggests that the larger the distance between the discontinuous wavy fins, the better the mixing of fluid on both sides of the fin, thereby enhancing the heat transfer performance. At the same time, the increase of breaking distance increases the swirl flow near the fin surface. Figure 10b indicates that the temperature increases at the breaking edge of the second row, which is mainly due to the discontinuous structure interrupting the development of fluid boundary layer and thermal fluid boundary. Figure 9c shows that the heat exchanger performance evaluation criteria for the discontinuous wavy fin with 1 mm spacing is highest.

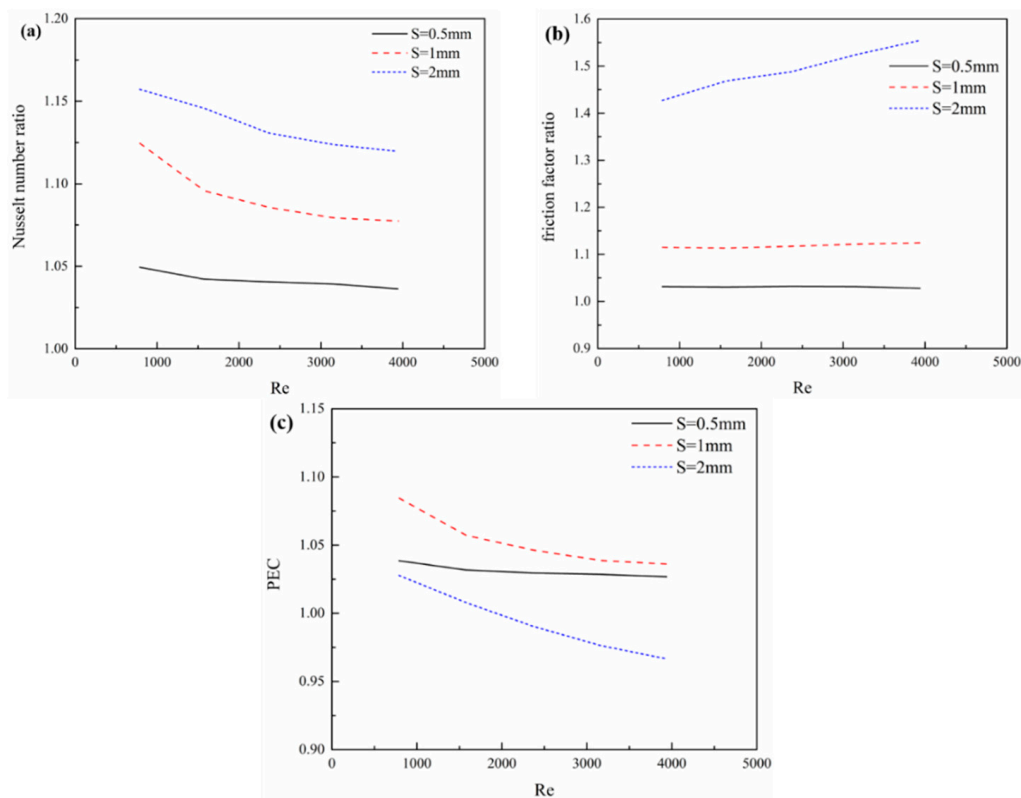


Figure 9. Influence of different breaking distance on heat transfer performance with Reynolds number. (a) Nusselt number ratio; (b) friction factor ratio; (c) the PEC.

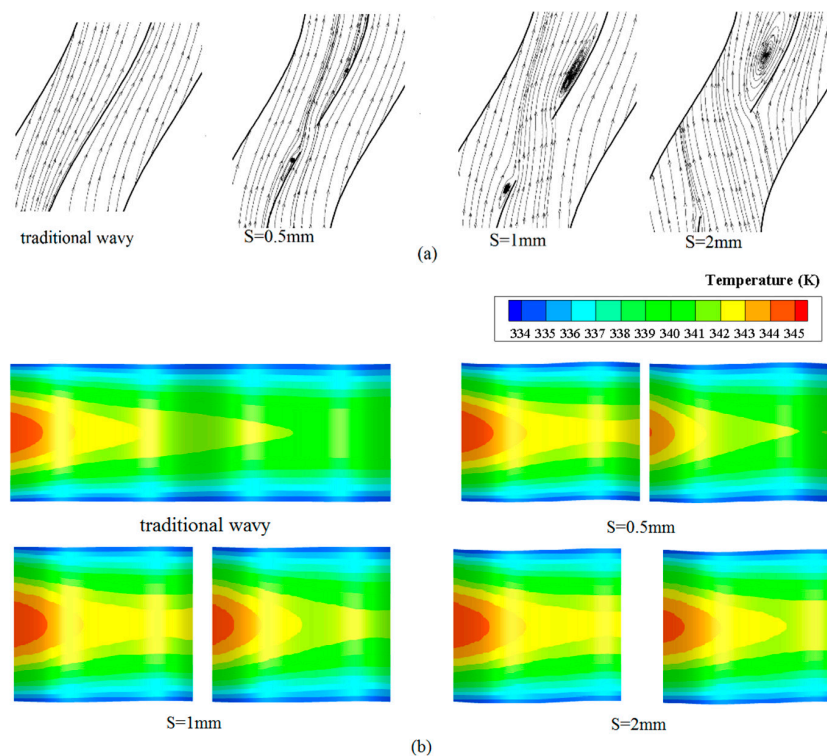


Figure 10. (a) Change in the streamline and (b) fin surface temperature distribution of the traditional wavy fin and discontinuous wavy fin when the breaking distances are 0.5 mm, 1 mm and 2 mm.

3.4. Influence of Waviness Aspect Ratio of Different Wavy Fin

According to the results of previous studies, the perforated wavy fin with $R = 1.5$ mm, staggered wavy fin with $\beta = 0.4$ and discontinuous wavy fin with $S = 1$ mm are chosen to compare with the traditional wavy fin at different waviness aspect ratio. Three values are considered ($\gamma = 0.38, 0.42$ and 0.45) to investigate the effects of the waviness aspect ratio.

The variations of the Nusselt number ratio ($Nu / Nu_{basic,wavy}$) over the three new kinds of wavy fins are shown in Figure 11a–c for different waviness aspect ratio. As it can be seen, all curves have values higher than 1 which indicate that the adopted techniques are beneficial for the heat transfer. It is found that the Nusselt number ratio of the perforated wavy fin with $r = 1.5$ mm increases with the increasing inlet velocity, and that of the discontinuous wavy fin remains almost constant slightly bigger than 1, while the Nusselt number ratio of staggered wavy fin decreases by increasing inlet velocity. Obviously, it can be also observed that the Nusselt number ratio of the perforated wavy fin with $r = 1.5$ mm is the highest in all cases. At the same time, with the increase of the waviness aspect ratio, the advantage of the perforated wavy fin is more obvious while that of the other two kinds of fins are slightly declining.

It indicates that the perforation and serration techniques are beneficial for the enhancement of heat transfer at different waviness aspect ratio. It is because the perforation and serration lead to collision among streamlines and thus the enhanced flow turbulence result in greater fluid mixing. Although the heat transfer performance of the discontinuous wavy fin is not much increased, the heat transfer area is reduced which is good for saving materials.

The variations of friction factor ratio ($f / f_{basic,wavy}$) for the three kinds of wavy fins against the inlet velocity are shown in Figure 12a–c for different waviness aspect ratios. At a given velocity, the friction factor ratio of the perforated wavy fin with $r = 1.5$ mm is the highest. This can be explained by strong flow fluctuation in the presence of holes on the fin surface. As can be seen, with the increase of the waviness aspect ratio, the friction factor ratio decreases. Especially for the discontinuous wavy fin, the friction factor ratio gradually becomes less than 1. The point is that the bigger waviness aspect

ratio causes stronger swirl flow near the fin surface, and this trend is stronger in the traditional wavy fin than in the staggered wavy fin and discontinuous wavy fin as shown in Figure 13.

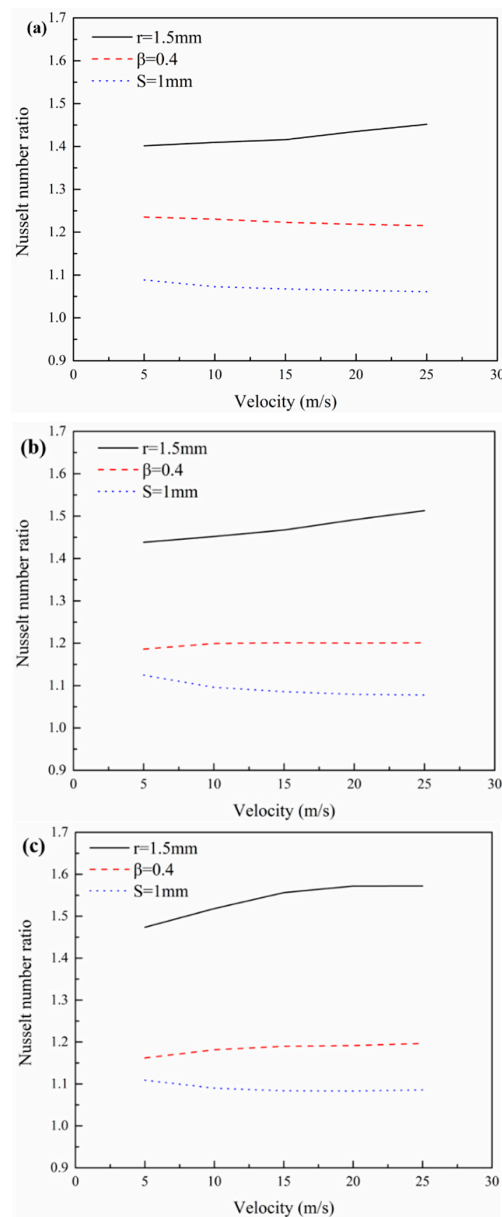


Figure 11. Nusselt number ratio versus the inlet velocity for three kinds of wavy fin with (a) $\gamma = 0.38$; (b) $\gamma = 0.42$; (c) $\gamma = 0.45$.

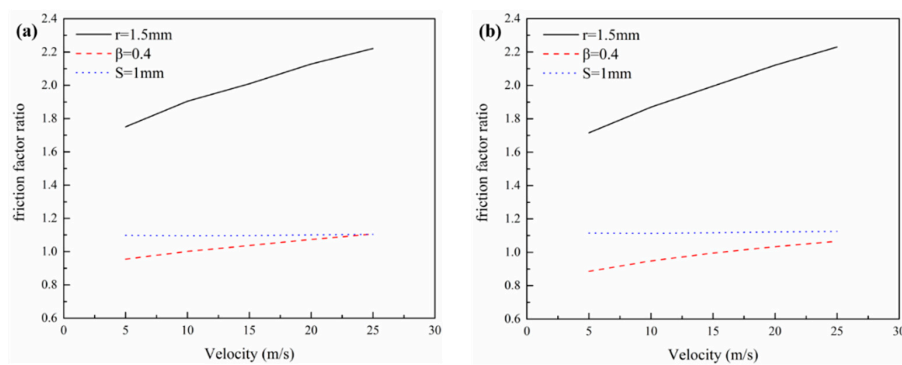


Figure 12. Cont.

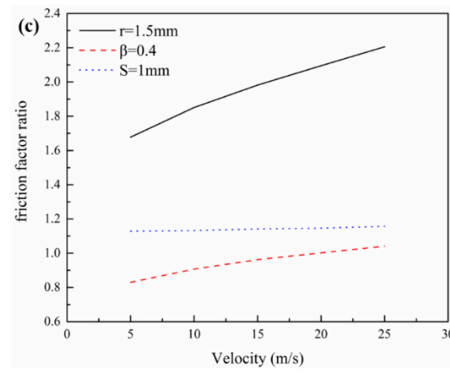


Figure 12. Friction factor ratio versus the inlet velocity for three kinds of wavy fin with (a) $\gamma = 0.38$; (b) $\gamma = 0.42$; (c) $\gamma = 0.45$.

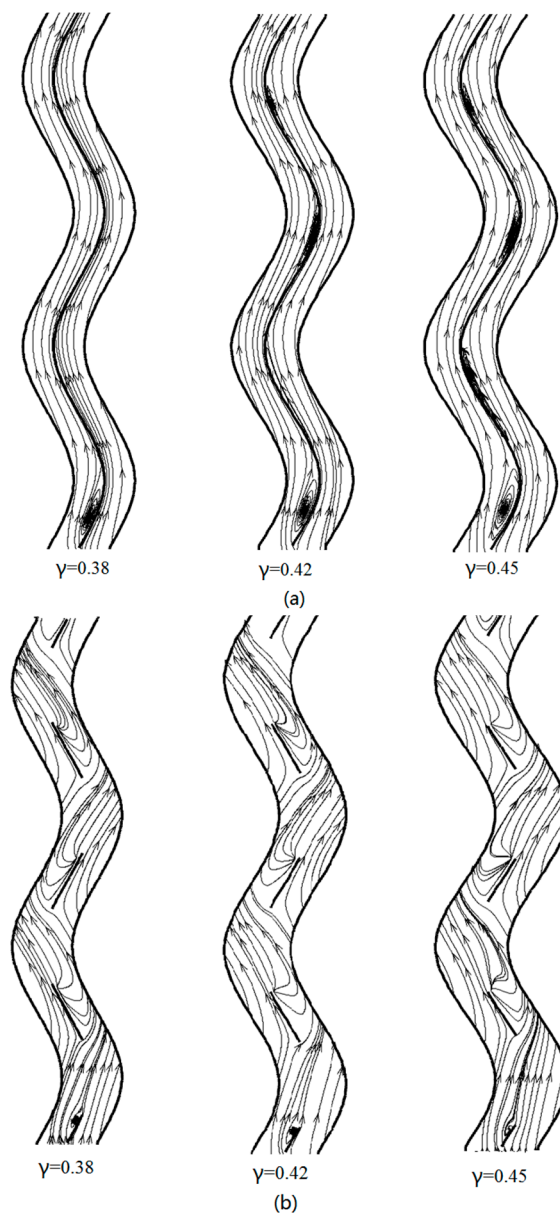


Figure 13. Cont.

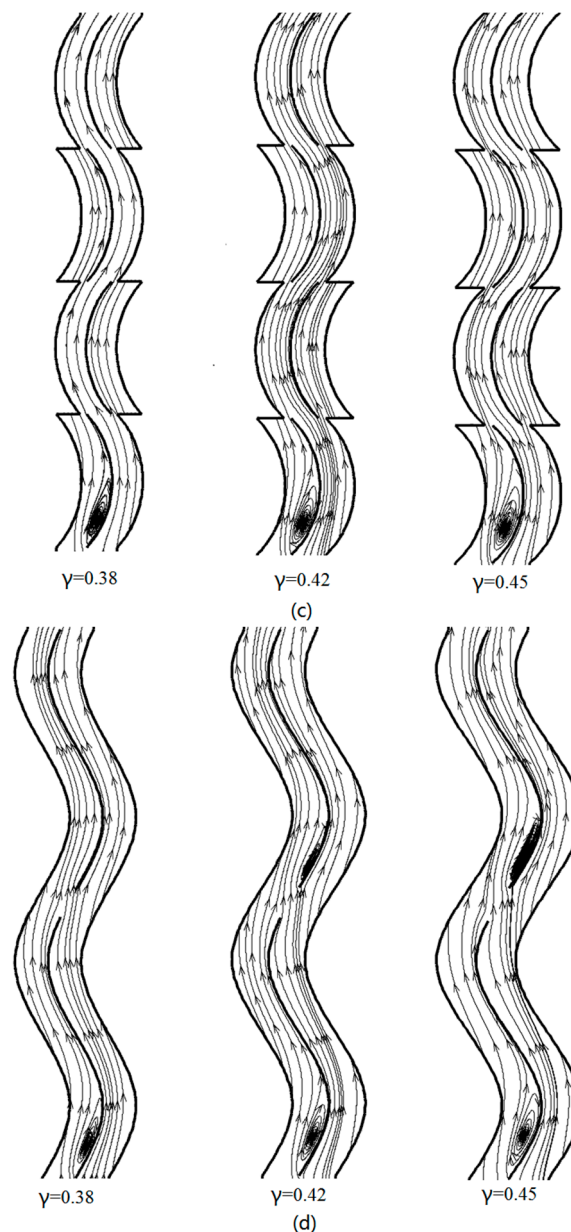


Figure 13. Change in the streamline of the (a) traditional wavy fin; (b) perforated wavy hole; (c) staggered wavy fin; and (d) discontinuous wavy fin when the waviness aspect ratio are 0.38, 0.42, and 0.45.

Figure 14a–c shows the variations of thermal-hydraulic performance factor over the three kinds of wavy fins for different waviness aspect ratio. The thermal-hydraulic performance factors of proposed wavy fins are all larger than 1. The change of thermal-hydraulic performance factor of the discontinuous wavy fin for different inlet velocity is small at different waviness aspect ratios. It is worth noting that with the increase of the waviness aspect ratio, the predominance of the staggered wavy fin is gradually surpassed by the perforated wavy fin. It means that using the serration technique in the smaller aspect ratio shows a considerable improvement in the thermal-hydraulic performance of the wavy fin. The maximum PEC of 1.24 is obtained for the perforated wavy fin at the largest waviness aspect ratio.

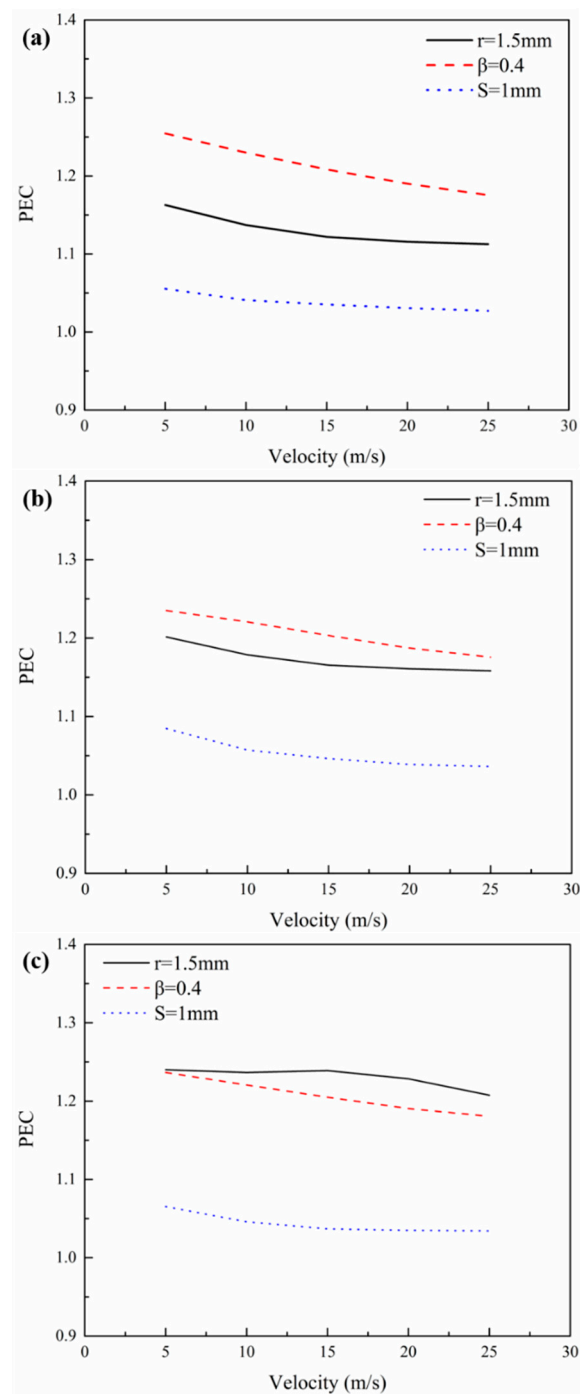


Figure 14. Thermal-hydraulic performance factor versus the inlet velocity for three kinds of wavy fin with (a) $\gamma = 0.38$; (b) $\gamma = 0.42$; (c) $\gamma = 0.45$.

4. Conclusions

Three new kinds of wavy plate fins, namely perforated wavy fin, staggered wavy fin and discontinuous wavy fin, are proposed and investigated by numerical simulation. The current study shows that the proposed perforation, serration, and breaking technology may have advantages over the traditional wavy fins. The following results obtained can be helpful to improve air-side heat transfer performance of the plate fin heat exchanger.

- For perforated wavy fin, the enlarged hole can strengthen the flow turbulence, causing rapid mixing between the core and the fluid near the fin surface. The bigger the holes, the better the thermal-hydraulic performance. For staggered wavy fin, the greater staggered ratio, the less flow turbulence at the staggered section. Then, the larger the staggered ratio, the better the thermal-hydraulic performance. For discontinuous wavy fin, the larger the distance between the discontinuous wavy fins, the better the mixing of fluid on both sides of the fin, thereby enhancing the heat transfer performance. At the same time, the friction factor has increased dramatically when the breaking distance is 2 mm.
- The Nusselt number and friction factor of the perforated wavy fin are all higher than that of the traditional wavy fin. The serration technology is beneficial to reduce the friction factor compared to the traditional wavy fin. Using the serration technique in the smaller aspect ratio can obviously improve the thermal-hydraulic performance of the wavy fin.
- At a given inlet velocity, Nusselt number and the PEC for the three proposed new wavy fins are higher than that of the traditional wavy fin, and it tends to almost invariable with increasing waviness aspect ratio for the discontinuous wavy fin. At the same time, with increasing of waviness aspect ratio, the PEC for the perforated wavy fin and staggered wavy fin increases. In addition, the predominance of the staggered wavy fin is gradually surpassed by the perforated wavy fin.
- The present research shows that the proposed heat transfer enhancement techniques all have advantages over the traditional wavy fin. Perforation is beneficial to the enhancement of the heat transfer and the improvement of the Nusselt number. Serration is beneficial to reduce the friction factor, and the breaking technique can reduce heat transfer area while enhancing heat transfer performance.

Author Contributions: Conceptualization, Z.G. and X.D.; Data curation, Y.X.; Investigation, Y.X.; Methodology, Z.G., X.D. and L.Y.; Supervision, X.D.

Acknowledgments: The financial supports for this research project from the National Natural Science Foundation of China (No. 51676069), the National Scientific and Technical Supporting Program of China (No. 2014BAA06B01) and the Fundamental Research Funds for the Central Universities of Ministry of Education of China (No. 2016XS34) are gratefully acknowledged.

Conflicts of Interest: The authors declare no conflict of interest. The founding sponsors had no role in the design of the study; in the collection, analyses, or interpretation of data; in the writing of the manuscript, and in the decision to publish the results.

Nomenclature

A	Total heat transfer area, m^2
A_c	Minimum free flow area, m^2
a	wave amplitude, mm
C_p	specific heat at constant pressure, $kJ/(kg \cdot K)$
D_h	hydraulic diameter, mm
F_c	Staggered spacing, mm
F_h	Fin height, mm
F_p	Fin pitch, mm
f	friction factor
G	mass velocity, $kg/(m^2 \cdot s)$
h	heat transfer coefficient, $W/(m^2 \cdot K)$
j	Colburn factor
k	The turbulence kinetic energy
L	Flow length, mm
L_z	Wavy fin passage length, mm
l	wavy length, mm
m	Mass flow rate, kg/s

Nu	Nusselt number
Pr	Prandtl number
p	pressure, Pa
PEC	Performance evaluation criteria
Q	Heat flow, W
r	Perforation radius, mm
Re	Reynolds number
S	Breaking distance in discontinuous wavy fin, mm; mean rate of strain tensor.
T	temperature, K
V	Air inlet velocity, m/s
u_i	Velocity in the i direction, m/s
u_j	Velocity in the j direction, m/s
x_i	Coordinate, m
<i>Greek Letters</i>	
β	Staggered ratio
γ	waviness aspect ratio
δ	Fin thickness, mm
δ_{ij}	Kronecker delta
η	Fin efficiency
λ	Thermal conductivity, W/(m·K)
μ	dynamic viscosity, Pa·s
μ_t	turbulent viscosity, Pa·s
ρ	Fluid density, kg/m ³
τ	Shear stress, Pa
<i>Subscripts</i>	
f	fin
in	inlet
out	outlet
p	plate
w	wall

References

1. Tinaut, F.V.; Melgar, A.; Ali, A.A.R. Correlations for heat transfer and flow friction characteristics of compact plate-type heat exchangers. *Int. J. Heat Mass Transf.* **1992**, *35*, 1659–1665. [[CrossRef](#)]
2. Ismail, L.S.; Velraj, R.; Ranganayakulu, C. Studies on pumping power in terms of pressure drop and heat transfer characteristics of compact plate-fin heat exchangers—A review. *Renew. Sustain. Energy Rev.* **2010**, *14*, 478–485.
3. Yousefi, M.; Enayatifar, R.; Darus, A.N. Optimal design of plate-fin heat exchangers by a hybrid evolutionary algorithm. *Int. Commun. Heat Mass Transf.* **2011**, *38*, 258–263. [[CrossRef](#)]
4. T'Joel, C.; Jacobi, A.; Paepe, M.D. Flow visualisation in inclined louvered fins. *Exp. Therm. Fluid Sci.* **2009**, *33*, 664–674. [[CrossRef](#)]
5. Vaisi, A.; Esmaeilpour, M.; Taherian, H. Experimental investigation of geometry effects on the performance of a compact louvered heat exchanger. *Appl. Therm. Eng.* **2011**, *31*, 3337–3346. [[CrossRef](#)]
6. Kays, W.M.; London, A.L. Compact heat exchangers. *J. Appl. Mech.* **1984**, *27*, 460–470. [[CrossRef](#)]
7. Khoshvaght-Aliabadi, M.; Hormozi, F.; Zamzamin, A. Role of channel shape on performance of plate-fin heat exchangers: Experimental assessment. *Int. J. Therm. Sci.* **2014**, *79*, 183–193. [[CrossRef](#)]
8. Du, J.; Qian, Z.Q.; Dai, Z.Y. Experimental study and numerical simulation of flow and heat transfer performance on an offset plate-fin heat exchanger. *Heat Mass Transf.* **2016**, *52*, 1–16. [[CrossRef](#)]
9. Dong, J.; Chen, J.; Zhang, W.; Hu, J. Experimental and numerical investigation of thermal-hydraulic performance in wavy fin-and-flat tube heat exchangers. *Appl. Therm. Eng.* **2010**, *30*, 1377–1386. [[CrossRef](#)]
10. Joardar, A.; Jacobi, A.M. Impact of leading edge delta-wing vortex generators on the thermal performance of a flat tube, louvered-fin compact heat exchanger. *Int. J. Heat Mass Transf.* **2005**, *48*, 1480–1493. [[CrossRef](#)]

11. Lotfi, B.; Sundén, B.; Wang, Q. An investigation of the thermo-hydraulic performance of the smooth wavy fin-and-elliptical tube heat exchangers utilizing new type vortex generators. *Appl. Energy* **2016**, *162*, 1282–1302. [[CrossRef](#)]
12. Tang, L.H.; Chu, W.X.; Ahmed, N.; Zeng, M. A new configuration of winglet longitudinal vortex generator to enhance heat transfer in a rectangular channel. *Appl. Therm. Eng.* **2016**, *104*, 74–84. [[CrossRef](#)]
13. Peng, H.; Xiang, L.; Li, J. Performance investigation of an innovative offset strip fin arrays in compact heat exchangers. *Energy Convers. Manag.* **2014**, *80*, 287–297. [[CrossRef](#)]
14. Alessa, A.H.; Maqableh, A.M.; Ammourah, S. Enhancement of natural convection heat transfer from a fin by rectangular perforations with aspect ratio of two. *Int. J. Phys. Sci.* **2009**, *4*, 540–547.
15. Shaeri, M.R.; Yaghoubi, M.; Jafarpur, K. Heat transfer analysis of lateral perforated fin heat sinks. *Appl. Energy* **2009**, *86*, 2019–2029. [[CrossRef](#)]
16. Ridouane, E.H.; Campo, A. Heat Transfer Enhancement of Air Flowing Across Grooved Channels: Joint Effects of Channel Height and Groove Depth. *J. Heat Transf.* **2008**, *130*, 281–293. [[CrossRef](#)]
17. Tian, L.; Liu, B.; Min, C.; Wang, J.; He, Y. Study on the effect of punched holes on flow structure and heat transfer of the plain fin with multi-row delta winglets. *Heat Mass Transf.* **2015**, *51*, 1523–1536. [[CrossRef](#)]
18. Du, X.; Feng, L.; Yang, Y.; Yang, L. Experimental study on heat transfer enhancement of wavy finned flat tube with longitudinal vortex generators. *Appl. Therm. Eng.* **2013**, *50*, 55–62. [[CrossRef](#)]
19. Lu, G.; Zhou, G. Numerical simulation on performances of plane and curved winglet type vortex generator pairs with punched holes. *Int. J. Heat Mass Transf.* **2016**, *102*, 679–690. [[CrossRef](#)]
20. Jeong, C.H.; Kim, H.R.; Ha, M.Y.; Son, S.W.; Lee, J.S.; Kim, P.Y. Numerical investigation of thermal enhancement of plate fin type heat exchanger with creases and holes in construction machinery. *Appl. Therm. Eng.* **2014**, *62*, 529–544. [[CrossRef](#)]
21. Ahn, H.S.; Lee, S.W.; Lau, S.C. Heat Transfer Enhancement for Turbulent Flow Through Blockages with Round and Elongated Holes in a Rectangular Channel. *J. Heat Transf.* **2007**, *129*, 1611–1615. [[CrossRef](#)]
22. Kays, W.M.; London, A.L. *Compact Heat Exchangers*, 3rd ed.; McGraw-Hill Book Company: New York, NY, USA, 1984.
23. Junqi, D.; Jiangping, C.; Zhijiu, C.; Yimin, Z.; Wenfeng, Z. Heat transfer and pressure drop correlations for the wavy fin and flat tube heat exchangers. *Appl. Therm. Eng.* **2007**, *27*, 2066–2073. [[CrossRef](#)]



© 2018 by the authors. Licensee MDPI, Basel, Switzerland. This article is an open access article distributed under the terms and conditions of the Creative Commons Attribution (CC BY) license (<http://creativecommons.org/licenses/by/4.0/>).